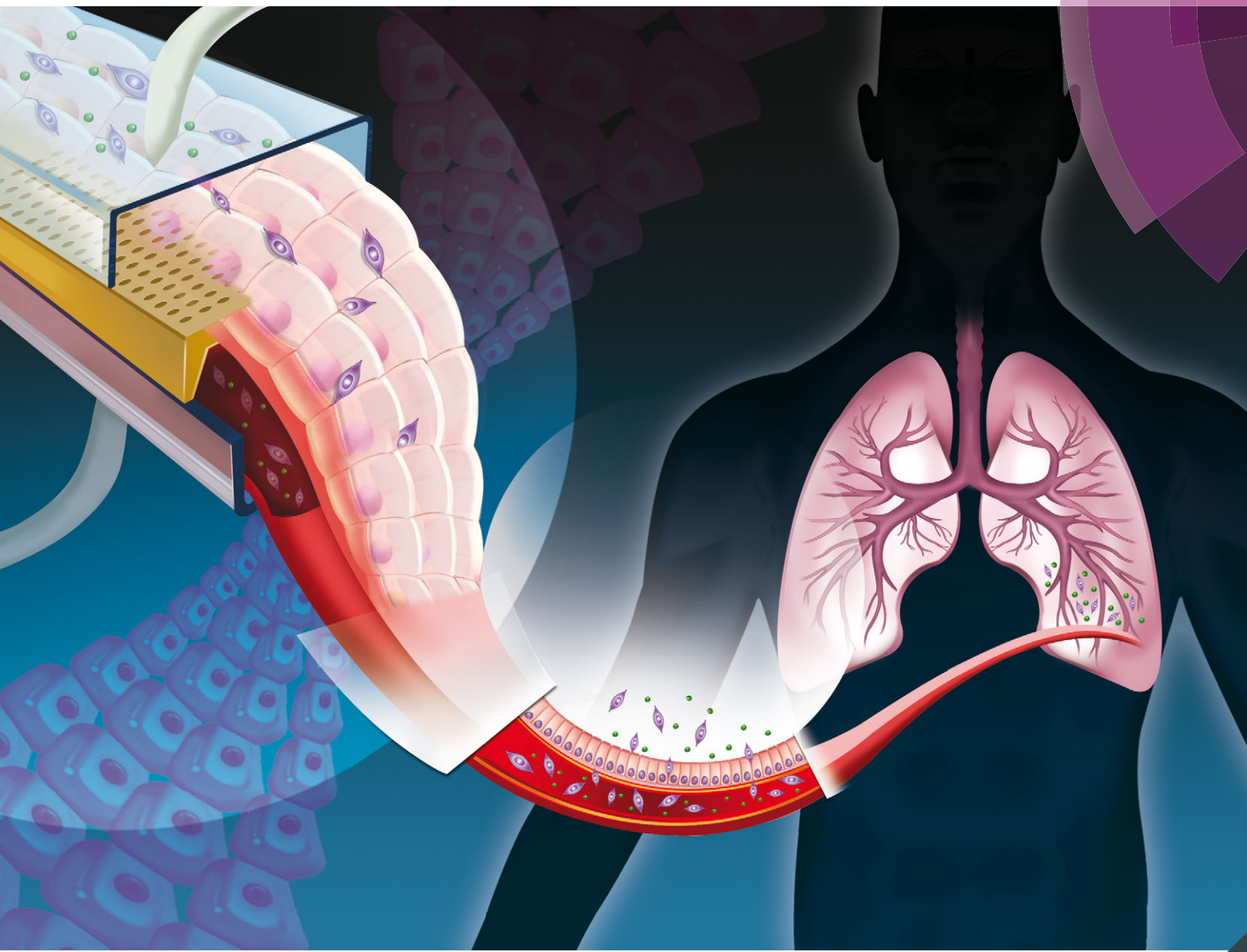


Integrative Biology

Interdisciplinary approaches for molecular and cellular life sciences

www.rsc.org/ibiology



ISSN 1757-9694



ROYAL SOCIETY
OF CHEMISTRY

PAPER

Cheng-Hsien Liu et al.

A biologically inspired lung-on-a-chip device for the study of protein-induced lung inflammation

Indexed in
Medline!



Cite this: *Integr. Biol.*, 2015,
7, 162

A biologically inspired lung-on-a-chip device for the study of protein-induced lung inflammation†

Tushar H. Punde,^a Wen-Hao Wu,^b Pei-Chun Lien,^c Ya-Ling Chang,^d Ping-Hsueh Kuo,^c Margaret Dah-Tsyr Chang,^c Kang-Yun Lee,^{def} Chien-Da Huang,^d Han-Pin Kuo,^d Yao-Fei Chan,^d Po-Chen Shih^b and Cheng-Hsien Liu*^b

This study reports a biomimetic microsystem that reconstitutes the lung microenvironment for monitoring the role of eosinophil cationic protein (ECP) in lung inflammation. ECP induces the airway epithelial cell expression of CXCL-12, which in turn stimulates the migration of fibrocytes towards the epithelium. This two-layered microfluidic system provides a feasible platform for perfusion culture, and was used in this study to reveal that the CXCL12–CXCR4 axis mediates ECP induced fibrocyte extravasation in lung inflammation. This ‘lung-on-a-chip’ microdevice serves as a dynamic transwell system by introducing a flow that can reconstitute the blood vessel–tissue interface for *in vitro* assays, enhancing pre-clinical studies. We made an attempt to develop a new microfluidic model which could not only simulate the transwell for studying cell migration, but could also study the migration in the presence of a flow mimicking the physiological conditions in the body. As blood vessels are the integral part of our body, this model gives an opportunity to study more realistic *in vitro* models of organs where the blood vessel *i.e.* flow based migration is involved.

Received 21st October 2014,
Accepted 30th November 2014

DOI: 10.1039/c4ib00239c

www.rsc.org/ibiology

Insight, innovation, integration

Eosinophil cationic protein (ECP) plays a major role in altering the pulmonary surfactant function and structure in asthma, leading to airway obstruction. ECP induces the airway epithelial cell expression of CXCL-12, which in turn stimulates the migration of fibrocytes towards the epithelium. This study reveals the role of CXCL12–CXCR4 axis mediating ECP induced fibrocyte extravasation in lung inflammation. Providing a more realistic approach, the lung-on-a-chip device provides an opportunity for airway remodeling by mimicking the bronchial epithelial lining for investigating the ECP-induced expression of CXCL12, resulting in the extravasation of fibrocytes. This model was designed to emphasize the role of ECP in lung inflammation and demonstrates a dynamic migration tool which also mimics the physiological flow conditions in the body.

Introduction

Animal studies, if assisted by innovative experimental model systems may reduce the time and expense involved in the

invention of pharmaceuticals. Developing microsystems that can mimic physiological conditions in the human body and maintain the spatiotemporal gradients would not only reduce the cost of drugs but would also expedite the invention process. The advancement of microfabrication technologies and their integration with microfluidics has allowed mimicking of the organ-level function in microdevices.^{1–4} For example, *in vitro* on-chip models of different organs such as the liver,^{5–8} blood vessels,^{9,10} kidney,^{11,12} bone,^{13,14} airways,^{15,16} brain,^{17–19} and gut^{20,21} at the microlevel facilitate the understanding of biological functions and disease mechanisms in detail.

Lung epithelium is a complex tissue where epithelial cells, subepithelial fibroblasts and the extracellular matrix of the airway wall are involved in the structure and function of the lung. During asthma, airway remodelling is characterized by shedding and derangement of epithelial cells, alteration in ECM deposition mediated by the functional interaction between the epithelium, lung fibroblasts and ECM in the underlying stromal

^a Institute of NanoEngineering and MicroSystems, National Tsing Hua University, Hsinchu, Taiwan, Republic of China

^b Department of Power Mechanical Engineering, National Tsing Hua University, Hsinchu, Taiwan, Republic of China. E-mail: liuch@pme.nthu.edu.tw; Tel: +886-3-5742496

^c Institute of Molecular and Cellular Biology, Department of Medical Science, National Tsing Hua University, Hsinchu, Taiwan, Republic of China

^d Pulmonary Medicine Research Center, Chang Gung Memorial Hospital, Linkou, Taiwan, Republic of China

^e Division of Pulmonary Medicine, Department of Internal Medicine, Shuang Ho Hospital, Taipei Medical University, Taipei, Taiwan, Republic of China

^f Department of Internal Medicine, Chang Gung University College of Medicine, Taoyuan, Taiwan, Republic of China

† Electronic supplementary information (ESI) available. See DOI: 10.1039/c4ib00239c

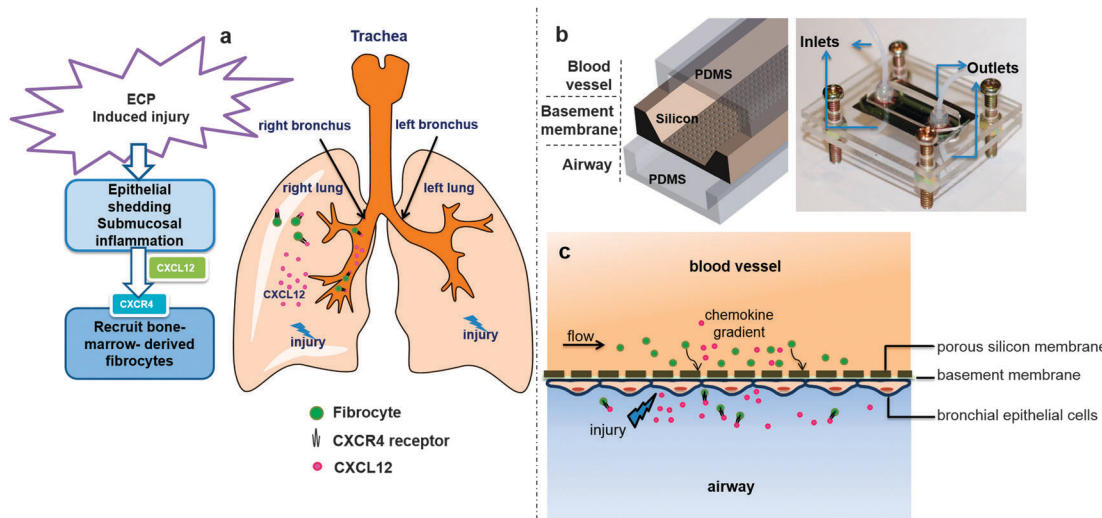


Fig. 1 (a) Predicted mechanism of ECP-induced fibrocyte migration during pulmonary fibrosis. When exposed to ECP, the epithelium lining in the airways stimulates a biochemical response, releasing chemokine (C–X–C motif) ligand 12 (CXCL12). CXCL12 diffuses to a blood vessel where it interacts with the chemokine (C–X–C motif) receptor 4 (CXCR4) expressed on fibrocytes, contributing to the migration of human peripheral blood fibrocytes into the airways. (b) A porous silicon membrane is sandwiched between two PDMS microchannels. The upper layer represents the blood capillary, whereas the bottom layer represents the airway. The chip is fitted on a chip holder with an inlet and outlet. (c) Schematic illustration of the ECP-induced fibrocyte migration on-chip, where the upper microfluidic channel serves as a blood vessel and the lower microfluidic channel represents the airway.

tissue.^{22,23} Asthmatic patients suffer from variable airflow obstruction and airway hyperresponsiveness, causing dyspnea, wheezing, and coughing.^{24,25} Infiltration of polymorphonuclear cells (mainly eosinophils) and mononuclear cells (mainly lymphocytes), and mast cells contribute to the early events of airway inflammation. Animal models have demonstrated that eosinophils contribute to airway remodelling in chronic asthma.²⁶ Eosinophil recruitment into tissues and its activation by cytokines results in the release of toxic proteins such as the major basic protein (MBP), eosinophil-derived neurotoxin (EDN), eosinophil cationic protein (ECP), and eosinophil peroxidase, thus causing airway tissue damage.²⁷ ECP in particular plays a major role in altering the pulmonary surfactant function and structure in asthma, which in turn may lead to airway obstruction.²⁸

Moreover, when the injured bronchial epithelial cells are stimulated with inflammatory cytokines, they release a crucial cytochemokine, chemokine (C–X–C motif) ligand 12 (CXCL12),²⁹ to recruit fibrocytes towards the injured epithelium. Fibrocyte infiltration in asthmatic airways is often correlated with airway remodelling and airway obstruction.^{30–33} It is well established that fibrocytes express the chemokine (C–X–C motif) receptor 4 (CXCR4), whereas the ligand, CXCL12 is produced by the bronchial epithelium, contributing to the migration of human peripheral blood fibrocytes.^{34,35}

Fibrocytes play a major role in airway inflammation, where fibrocytes are induced by increased expression of CXCL12.³³ The role of CXCL12–CXCR4 axis^{29,34} in fibrocyte migration has been well established. This work clearly demonstrates the role of ECP induced airway epithelial cell expression of CXCL12 and further migration of fibrocytes on the microfluidic chip which mimics the lung microenvironment. The predicted mechanism of the ECP-induced airway epithelial cell expression

of CXCL12, which in turn stimulates the migration of fibrocytes towards the epithelium, is illustrated in Fig. 1(a) and (c).

Regardless of the complex biological process involved in airway remodelling, this microfluidic device provides an opportunity for airway remodelling by co-culture of different cells. Though at this stage the co-culture model has not been demonstrated, this device mimics the bronchial epithelial lining for investigating the ECP-induced expression of CXCL12, resulting in the extravasation of fibrocytes. The microfluidic chip was fabricated by sandwiching a micropore array silicon chip between two polydimethylsiloxane (PDMS) channels (Fig. 1(b)). The silicon chip was fabricated by etching $5\text{ }\mu\text{m} \times 5\text{ }\mu\text{m}$ holes. The detailed fabrication procedure is displayed in the Fig. S1 (ESI†). The upper channel represented the circulatory system, whereas in the lower channel, the micropores were coated with fibronectin to enhance the adhesion of bronchial epithelial Beas-2B cells, and cultured, thus mimicking the bronchial environment (Fig. 1(c)) to demonstrate the lung-on-a-chip device. The detail experimental process is illustrated in Fig. S2 (ESI†).

Materials and methods

Cell culture

Beas-2B (ATCC® number: CRL-9609™) is a human bronchial epithelial cell line infected with an adenovirus (12-SV40 hybrid virus; Ad12SV40). Beas-2B cells were cultured in RPMI1640 medium (Sigma-Aldrich) supplemented with 65 °C heat-inactivated 10% (v/v) foetal bovine serum (FBS) (Gibco/Invitrogen) and 1% (v/v) PSA (penicillin, streptomycin, and amphotericin; Biosera). The cells were incubated under a humidified atmosphere of 5% CO₂ and 95% air.

For obtaining the subcultures, Beas-2B cells cultured in T75-flasks were removed from the humidified atmosphere to a laminar flow, and washed with 10 mL phosphate buffer solution (PBS) without $\text{Ca}^{2+}/\text{Mg}^{2+}$. Subsequently, 1.5 mL trypsin/EDTA [0.05%/0.02% (w/v)] (BIOCHROM AG) was pipetted onto the washed cell monolayer, and transferred into an incubator at 37 °C for 5 min. After trypsin treatment, the cells were suspended in 8.5 mL of a fresh serum-containing medium to inactivate trypsin, and 10–20 μL cells were seeded for cell count. The cells were transferred to T75-flasks containing a prewarmed medium, and adjusted to a final volume of 10 mL. The Beas-2B cells were cultured for 2 or 3 days depending on the cell density in the flask.

Purification of circulating fibrocytes

Human fibrocytes were isolated according to the method modified from a previous report.³⁴ Peripheral blood mononuclear cells (PBMCs) were isolated using the Ficoll Paque (GE Healthcare, Bio-science AB, Sweden) density gradient method. PBMCs were then transferred onto 10 cm culture dishes containing DMEM supplemented with 20% FCS, penicillin, streptomycin, and L-glutamine for 5 days. Nonadherent cells were discarded. The remaining adherent cells were cultured for another 7–10 days in a fresh medium. The fibrocytes were then purified using an immunomagnetically negative selection method to deplete B lymphocytes (anti-CD19 microbeads), T lymphocytes (anti-CD2 microbeads), and monocytes (anti-CD14 microbeads, MACS Miltenyi Biotec GmbH, Bergisch Gladbach, Germany). The purity of the fibrocytes was generally greater than 90%, as determined using FACS analysis after staining with CD45, Collagen I, and CD34. This study was approved by the ethical review board of Chang Gung Memorial Hospital (CGMH IRB No. 97-2245A3), and informed consent was obtained from all subjects.

Recombinant ECP

The *E. coli* harbouring the recombinant plasmid encoding human *ecp* with a hexahistidine tag (*ecp-6h*) was seeded into Terrific Broth (TB), and incubated at 37 °C for 4 h. Subsequently, 0.5 $\mu\text{g mL}^{-1}$ of IPTG was added to induce the expression of recombinant mature ECP-His. After 5 h bacteria were harvested by centrifugation at 2900 $\times g$ for 30 min at 4 °C, and the supernatant was discarded. An Ni Sepharose™ (GE Healthcare) was used to purify the ECP-6His. The denatured protein collected was added to 80 mM reduced-form-glutathione (GSH), and incubated at 25 °C for 2 h to facilitate the formation of disulphide bonds. After incubation, the protein was added dropwise to 100 times the volume of an ice-cold refolding buffer (pH 8.5) containing 0.2 mM oxidised-form-glutathione (GSSG), 0.5 M arginine, 20 mM Tris-HCl, 10% (v/v) glycerol, and was incubated at 4 °C for at least 36 h. After incubation, the refolded protein was condensed to a volume of approximately 10 mL. The proteins were then dialyzed to PBS, and the product was concentrated to approximately 1 mg mL^{-1} in an Amicon® Ultra-15 centrifugal filter devices equipped with a 3 K cut-off membrane (Millipore). The protein concentrations of the samples were determined using a BCA assay (Thermo, USA), using BSA as the standard.

RT-PCR and quantitative real-time PCR

Total RNA was isolated from Beas-2B cells, using the TRIZOL reagent (Invitrogen, Carlsbad, CA), following the instructions of the manufacturer. One microgram of total RNA was then reverse-transcribed into cDNA with Moloney murine leukaemia virus (M-MLV) reverse transcriptase (Invitrogen) and oligo-dT primers (Invitrogen) in a 20 μL reaction. β -Actin cDNA amplification was used as an internal control. PCR products were separated on 1.5% agarose gel, and visualised using ethidium bromide staining. When required, the PCR products were purified from agarose gels, using a QIAquick gel extraction kit (Qiagen Inc., Valencia, CA). Direct sequencing of the purified PCR products was performed using an ABI-PRISM model 377 sequencer (PE Applied Biosystems, Foster City, CA). Alternatively, PCR products were cloned using a pCR II-TOPO TA cloning kit (Invitrogen), and sequenced with T7 and Sp6 primers. The sequences were aligned with the corresponding database provided by the National Center for Biotechnology Information (Bethesda, MD). Quantitative real-time RT-PCR was performed as follows: for each reaction, 2 μL of cDNA, 10 μL of 2 \times Power SYBR Green PCR Master Mix reagent (Applied Biosystems), 2 μL of the primer pair, and 6 μL of distilled water was mixed. PCR was performed on an ABI PRISM 7500 real-time PCR system. The C_t values of test genes were calculated by normalising that of the internal control housekeeping gene β -actin or GAPDH. The gene expression level was calculated using the test mRNA expression.

Human CXCL-12 enzyme-link immunosorbent assay (ELISA)

Human CXCL-12 was quantitatively measured in cell culture supernatants, using a CXCL-12 ELISA kit (Abcam ab100637) with an antibody specific for human CXCL-12, coated on a 96-well plate. The wells were incubated with 100 μL of the standard or sample for 2.5 h at room temperature. After washing with 1 \times wash solution four times, 100 μL of antibiotin antibody was added into each well. After washing, 100 μL of streptavidin solution was incubated for 45 h at room temperature. After washing, 100 μL of TMB One-Step Substrate Reagent was added into each well, and incubated for 30 min at room temperature. Finally, Stop Solution (50 μL) was added into each well, and read immediately using a spectrophotometer at 450 nm.

Transwell assay

Beas-2B cells were cultured on a 24-well plate at 37 °C for 24 h and stimulated with 16 $\mu\text{g mL}^{-1}$ and 80 $\mu\text{g mL}^{-1}$ refold ECP-6His at 37 °C for 12 h and 24 h separately. Fibrocytes labelled with carboxyfluorescein succinimidyl ester (CFSE) were seeded in transwells (BD 353097, 8 μm pores), and incubated at 37 °C for 3 h, 6 h, 12 h and 24 h, separately. In antibody-blocking experiments, before the fibrocytes were transferred to the transwell system, 2.5 $\mu\text{g mL}^{-1}$ of the CXCR4 antibody (R&D, MAB 170) was used to block the CXCR4 receptor on fibrocytes at 37 °C for 1 h. After the Beas-2B cells were treated with ECP-6His for 12 h and 24 h, the CXCR4-blocked fibrocytes were injected into transwells, and incubated at 37 °C for 12 h and 24 h

separately. For all of the experiments, the data were quantified by counting the number of cells per microscopic field at a 10-fold magnification.

Results and discussion

ECP-6His effects on mRNA and protein expression of CXCL-12 in Beas-2B cells

Based on the proposed mechanism of ECP-induced migration of fibrocytes during bronchial inflammation (Fig. 1a), real-time PCR and ELISA were used to perform quantitative analyses of mRNA and protein expression separately. In this study, the mRNA expression of CXCL-12 at various time points was measured using real-time reverse-transcription PCR (RT-PCR) to screen the appropriate period for treatment with ECP-6His, and specific periods for observing fibrocyte migration.

Beas-2B cells were cultured in 60 mm dishes for 24 h and starved for 24 h in a serum-free medium. Subsequently, 5 μ M (80 μ g mL $^{-1}$) ECP-6His was added at 37 °C for 3 h, 6 h, 12 h and 24 h, and gene expression was measured by real-time RT-PCR. Compared with the control group, for Beas-2B cells treated with ECP-6His at 3 h, 6 h, 12 h, and 24 h, the mRNA expression of CXCL-12 was elevated by 1.7-fold, 3.5-fold, 4.7-fold, and 2.6-fold, respectively, indicating that the mRNA expression of CXCL-12 reached the maximum at 12 h, and gradually decreased until 24 h (Fig. 2a). In addition, given the significant differences in gene expression, the cell culture medium was separately collected to analyse the amount of target protein (CXCL-12), using an ELISA kit. Upon treatment with 80 μ g mL $^{-1}$

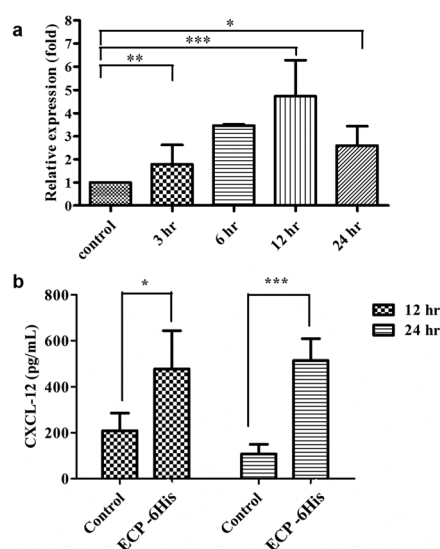


Fig. 2 ECP-6His effects on mRNA and protein expression of CXCL-12. (a) CXCL-12 mRNA was quantified using RT-PCR after 3 h, 6 h, 12 h, and 24 h in 60 mm dish separately; data are expressed as relative fold expression, with the mock-treated sample set at one. (b) CXCL-12 protein levels in the culture medium were measured using an ELISA kit. The control represents the Beas-2B cells without ECP treatment. The data represent at least three independent experiments, and the error bars indicate standard deviation (SD) (* $p < 0.01$, ** $p < 0.005$, *** $p < 0.001$). (Concentration of ECP-6His is 80 μ g mL $^{-1}$.)

ECP-6His for 12 h and 24 h, protein expression of CXCL-12 increased by 2.3-fold in 12 h and 4.8-fold in 24 h, compared with the control group (Fig. 2b), demonstrating that refold ECP-6His induced CXCL-12 in the Beas-2B cells at both mRNA and protein expression levels. According to these results, the Beas-2B cells treated with ECP-6His began synthesising the CXCL-12 protein at 6 h, and released it to the extracellular medium at 12 h.

Fibrocyte migration towards ECP-6His-stimulated Beas-2B cells in the transwell system

To prove our hypothesis (Fig. 1a), first, we used a traditional migration assay (*i.e.*, transwell system) to demonstrate fibrocyte migration towards Beas-2B cells on ECP-6His stimulation. The Beas-2B cells were cultured and then stimulated with 80 μ g mL $^{-1}$ ECP-6His for 12 h and 24 h separately. After treating with ECP-6His, fibrocytes were injected into the transwell, and incubated at 37 °C for 3 h, 6 h, 12 h and 24 h separately. More fibrocytes migrated towards the Beas-2B cells after 12 h and 24 h than after 3 h and 6 h of treatment (Fig. 3a and b), suggesting a time-dependent variation from 3 h to 12 h, but no significant difference was observed between 12 h and 24 h, because the expression of CXCL-12 reached a steady state.

These results revealed that ECP-6His was responsible for recruiting fibrocytes towards Beas-2B cells in the transwell system. To confirm the role of ECP-6His in the induction of fibrocyte migration towards Beas-2B cells as a result of chemotactic attraction of CXCL-12, the CXCR4 antibody was used to block the CXCR4 receptor on fibrocytes. After the Beas-2B cells were stimulated with 80 μ g mL $^{-1}$ ECP-6His for 12 h and CXCR4-blocked fibrocytes were injected, a 53% decrease in fibrocyte migration was observed (Fig. 4a). On treatment with 80 μ g mL $^{-1}$ ECP-6His for 24 h, fibrocyte migration decreased by

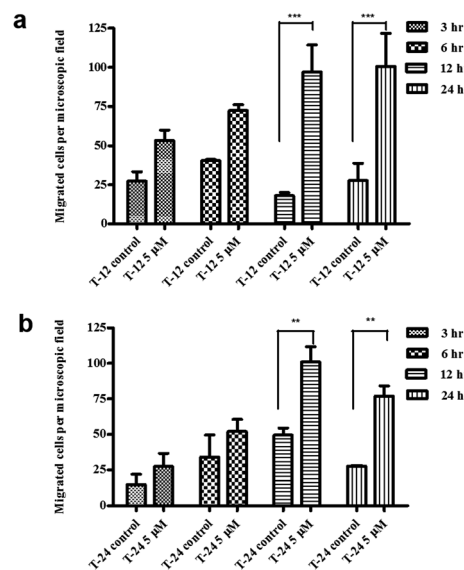


Fig. 3 ECP-induced fibrocyte migration per microscopic field on the transwell system. The number of fibrocytes migrating through the membrane pores was quantified by counting the fluorescent cells (* $p < 0.01$, ** $p < 0.005$, *** $p < 0.001$). T is the treatment time (h) of ECP-6His.

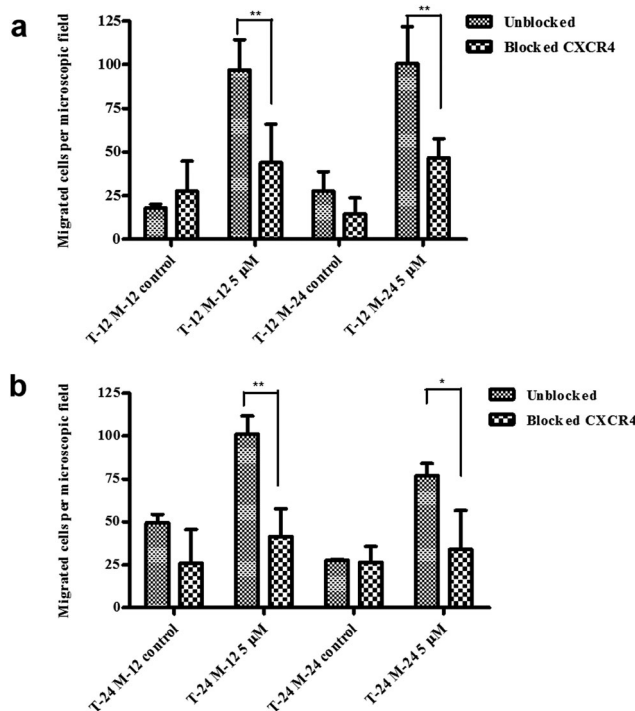


Fig. 4 ECP-induced fibrocyte migration blocked with the CXCR4 antibody per microscopic field on the transwell system. The number of fibrocytes migrating through the membrane pores was quantified by counting the fluorescent cells. The CXCR4 antibody was used to block fibrocytes, and the unblocked group was the control (*T*, treatment time of ECP-6His; *M*, migration time of fibrocytes; **p* < 0.01, ***p* < 0.005, ****p* < 0.001).

50% for 12 h and 24 h because of the blocking of the CXCR4 receptor (Fig. 4b). Compared with unblocked fibrocytes, these data revealed that CXCL-12, which was released from Beas-2B cells, leading to the transmigration of fibrocytes, was a critical chemokine. To sum up, the gene and protein expression of CXCL-12 demonstrated the effect of ECP-6His treatment on Beas-2B cells, contributing to the release of CXCL-12, and further migration of fibrocytes towards the injured bronchial epithelium, thus establishing the biological mechanism of airway inflammation. To confirm this mechanism, additional experiments were conducted on the lung-on-a-chip device which mimics the lung-like conditions.

Fibrocyte transmigration towards Beas-2B cells treated with ECP-6His on the lung-on-a-chip device

The microfluidic chip system was designed to mimic the physiological conditions in human airways for studying asthmatic inflammation. Taking advantage of the microfluidic platform, the chip served like a dynamic transwell where fibrocyte migration could be evaluated under real-time conditions.

For establishing the mechanism of the *in vitro* immune response in bronchial microenvironments, Beas-2B cells were cultured on a micropore array silicon chip for 24 h to form a confluent layer, thus mimicking the airway microenvironment. The Beas-2B cells were further stimulated with 80 $\mu\text{g mL}^{-1}$ ECP-6His for 12 h and 24 h separately, which in turn released

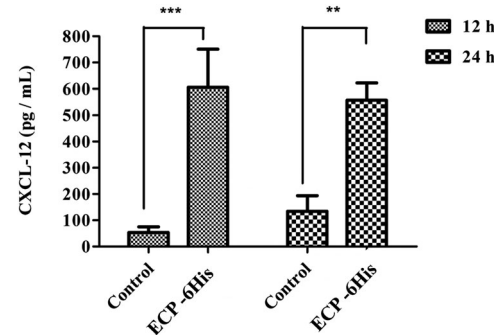


Fig. 5 ECP-6His effect on the protein expression of CXCL-12 in the microfluidic chip. Beas-2B cells were cultured in the microfluidic chip for 24 h, followed by stimulation with 80 $\mu\text{g mL}^{-1}$ ECP-6His at 37 °C for 12 h and 24 h separately, and the cell culture supernatant was collected. The CXCL-12 levels in the culture medium were measured by following standard ELISA kit procedures (***p* < 0.005, ****p* < 0.001).

CXCL-12 to recruit fibrocytes towards the airway. The used culture medium was collected from the microfluidic chip for investigating the presence of the target protein by using a standard CXCL-12 ELISA kit; the outcomes are illustrated in Fig. 5. No substantial difference in the CXCL-12 protein expression was detected after 12 h and 24 h of ECP-6His treatment.

To substantiate the immune responses, after the Beas-2B cells were treated with 80 $\mu\text{g mL}^{-1}$ ECP-6His for 12 h and 24 h separately, fibrocytes were loaded onto the reverse side of the Beas-2B cells lining at a continuous 160 $\mu\text{m s}^{-1}$ flow rate (which is similar to the flow rate in human blood capillaries). For the control group, when the cells were treated with serum free media, with time serum deprivation induces apoptotic cell death and leads to a decrease in the cell number (Fig. 6c). For the experimental group, it is observed that ECP inhibits the viability of Beas-2B cells and induces apoptosis (Fig. 6d-f).³⁶

Subsequently, after 3 h, 6 h, 12 h and 24 h, bright field and fluorescence images (20 \times objective) were taken to observe fibrocyte extravasation in pulmonary inflammation (Fig. 6c-f). Fibrocyte migration was triggered by immune cytokines released from the Beas-2B cells treated with 80 $\mu\text{g mL}^{-1}$ ECP-6His for 12 h, and substantial effects were observed when the Beas-2B cells were cultured in a serum-free medium.

Thus, ECP-6His induced pulmonary immune responses in the Beas-2B cells, contributing to the release of CXCL-12 to recruit fibrocytes towards injured tissues. Fig. 6(c) reveals that fibrocytes started to transmigrate towards the Beas-2B cells at 3 h, and a substantial difference between the control and experimental group was observed after 12 h of transmigration.

Because of the continuous flow rate in the proposed device, the fibrocytes persistently experienced a CXCL-12 concentration gradient during the immune response, and migrated towards the Beas-2B cells. Fig. 6(d) and (f) exhibit no considerable differences in the number of migrated fibrocytes, presumably due to the fact that CXCL-12 expression reached a steady state (Fig. 5). The fibrocyte migration data in Fig. 6a and b show that the number of fibrocytes that migrated to the bottom channel for 12 h and 24 h was considerably greater than those observed after 3 h and 6 h.

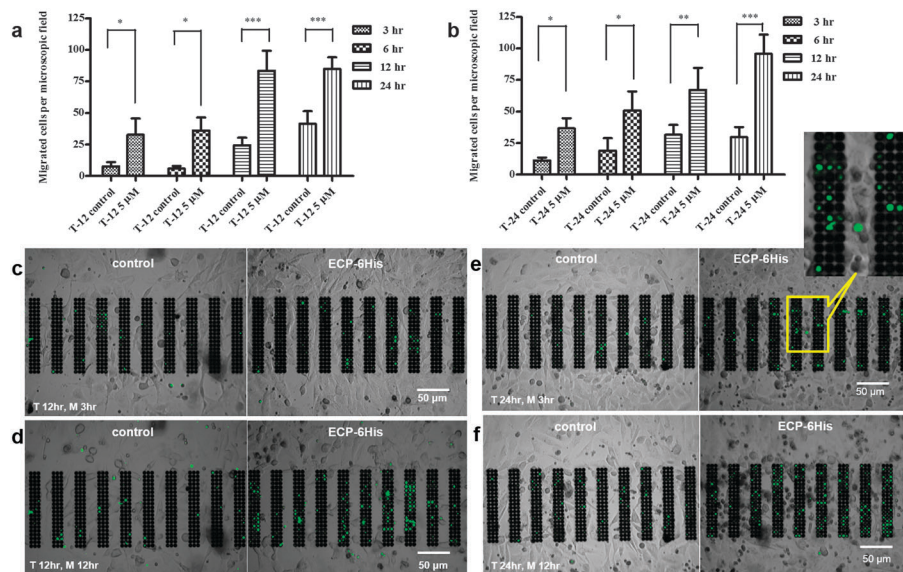


Fig. 6 Fibrocyte migration in micro-fluidic lab chip system. (a) and (b) Number of fibrocytes migrated per microscopic field at a flow rate of $160 \mu\text{m s}^{-1}$ on the lung-on-a-chip system. Migrated fibrocytes were counted from real-time fluorescence images taken at 12 h and 24 h treatment with ECP-6HIs. Fibrocyte extravasation at $160 \mu\text{m s}^{-1}$ for 3 h, 6 h, 12 h and 24 h was separately analysed to determine the significant differences between the control and experimental groups ($*p < 0.01$, $**p < 0.005$, $***p < 0.001$). T is the treatment time (h) of ECP-6HIs. (c)–(f) Images depict Beas-2B cells cultured in the microfluidic device and via fibrocyte extravasation. Beas-2B cells were cultured at 37°C and treated with serum free medium (*i.e.*, control) and $80 \mu\text{g mL}^{-1}$ ECP-6HIs at 37°C for 12 h and 24 h in separate microdevices. Bright field and fluorescence images were taken and merged for observing real time fibrocyte extravasation after 3 h and 12 h (T : treatment time; M : migration time). The zoomed section shows the fibrocytes at different migration stages. Some fibrocytes have started to appear and some have completely migrated into the airway channel.

Based on the proposed mechanism of cytokine-induced airway subepithelial fibrosis, RT-PCR and ELISA were used for quantitatively analysing mRNA and protein expression separately. The results showed that CXCL-12, a ligand for CXCR4, was responsible for recruiting fibrocytes to the lung, and was involved in inflammation.³⁷ Beas-2B cells treated with refold ECP-6HIs exhibited elevated CXCL-12 mRNA expression levels, followed by the steady state condition. Thus, the CXCL-12 secreted from the Beas-2B cells played a crucial role in inflammation.

Conclusion

The ‘lung-on-a-chip’ microfluidic device is useful for investigating the role of ECP in airway remodelling (*e.g.*, subepithelial fibrosis), thus linking ECP, CXCL12 and CXCR4 responsible for fibrocyte extravasation in lung inflammation. ECP plays a major role in attracting fibrocytes from blood vessels to airways. ECP stimulates the Beas-2B cells to produce CXCL 12, which in turn attracts the fibrocytes, thus contributing to the inflammatory conditions. A high number of attracted fibrocytes not only indicates the inflammatory conditions in the airway but also contributes to severe fibrotic conditions in the epithelium. The quantitative results of fibrocyte migration obtained by using our chip (Fig. 6a) are similar to those obtained by using the transwell assay (Fig. 3) which affirms the validity of the microfluidic device.

The porous silicon membrane sandwiched between two microfluidic channels offers a platform for physiological mass

transport for optimizing cell growth. The 3D microfluidic chip platform could provide a perfusion-based microenvironment for long-term culture with medium renewal, whereas in the transwell the culture medium is supplied in a batch-wise manner. In the case of transwell inserts, though we might culture epithelial cells on the bottom of transwell inserts, it is not possible to continuously perfuse fresh medium to the cells. Besides, the flow phenomenon cannot be imagined on the transwell if more complex experiments are to be carried out. In the case of our microfluidic chip with the porous silicon membrane, different cell media can be easily supplied/controlled in each microfluidic channel mimicking the *in vivo* situation. Different types of cells could also be cultured on both sides of the porous silicon membrane.

This device also enables prolonged migration study as the chemokine gradient can be maintained throughout the experiment but in the case of a transwell the test-agent concentration quickly equalises in the compartment below and above the membrane. Due to the use of transparent PDMS material, both the top and bottom microfluidic channels serve as windows for live cell imaging when using an inverted microscope. Silicon membrane sandwiched between the two microchannels provides the advantage of non-transparency, as it blocks the unnecessary fluorescence of non-migrated cells from the opposite channel allowing real-time imaging of fibrocyte extravasation while maintaining the *in vitro* spatiotemporal gradient.

When compared with the *in vivo* situation, the lung-on-a-chip device presented here lacks several structural and biological components (lung fibroblast, immune cells like eosinophils

and lymphocytes) that are crucial for investigating the complex pathophysiology of asthma. However, this model was designed to emphasize the role of ECP in lung inflammation and demonstrate a dynamic migration tool which mimics the physiological flow conditions in the body. Though at this stage the effect of the flow on migration has not been studied, it would be interesting to study the cell-cell interaction during the course of the flow and its possible effect on migration. As blood vessels are an integral part of organs and tissues, the chip model could provide a feasible platform to mimic the flow conditions of the blood vessel when studying the specific features of the organs where blood vessels are an integral part. Moreover this model presents an innovative approach for doing migration assays and concurrent cell-cell interactions, thus enhancing the capability of migration assays when more advanced and complex migration assays are to be done.

Acknowledgements

This project was financially sponsored by the Chang Gung Medical Hospital-Tsinghua Research Program (Grant No. 100N2713E1) and the National Science Council (Grant No. 99-2221-E-007-125-MY3). We acknowledge Prof. Hwan-You Chang and his research group in the Microbiology and Biotechnology Laboratory at the National Tsing Hua University for the helpful discussions on research development.

References

- 1 H. Peng and E. L. Herzog, Fibrocytes: emerging effector cells in chronic inflammation, *Curr. Opin. Pharmacol.*, 2012, **12**, 491–496.
- 2 D. Huh, Y. S. Torisawa, G. A. Hamilton, H. J. Kim and D. E. Ingber, Microengineered physiological biomimicry: organs-on-chips, *Lab Chip*, 2012, **12**, 2156–2164.
- 3 J. H. Sung and M. L. Shuler, Microtechnology for mimicking *in vivo* tissue environment, *Ann. Biomed. Eng.*, 2012, **40**, 1289–1300.
- 4 A. D. van der Meer and A. van den Berg, Organs-on-chips: breaking the *in vitro* impasse, *Integr. Biol.*, 2012, **4**, 461–470.
- 5 C.-T. Ho, R.-Z. Lin, W.-Y. Chang, H.-Y. Chang and C.-H. Liu, Rapid heterogeneous liver-cell on-chip patterning via the enhanced field-induced dielectrophoresis trap, *Lab Chip*, 2006, **6**, 724–734.
- 6 S.-A. Lee, D. Y. No, E. Kang, J. Ju, D.-S. Kim and S.-H. Lee, Spheroid-based three-dimensional liver-on-a-chip to investigate hepatocyte-hepatocytic stellate cell interactions and flow effects, *Lab Chip*, 2013, **13**, 3529–3537.
- 7 S. R. Khetani and S. N. Bhatia, Microscale culture of human liver cells for drug development, *Nat. Biotechnol.*, 2008, **26**, 120–126.
- 8 C. T. Ho, R. Z. Lin, R. J. Chen, C. K. Chin, S. E. Gong, H. Y. Chang, H. L. Peng, L. Hsu, T. R. Yew, S. F. Chang and C. H. Liu, Liver-cell patterning Lab Chip: mimicking the morphology of liver lobule tissue, *Lab Chip*, 2013, **13**, 3578–3587.
- 9 C. Franco and H. Gerhardt, Tissue engineering: Blood vessels on a chip, *Nature*, 2012, **488**, 465–466.
- 10 M. L. Moya, Y. H. Hsu, A. P. Lee, C. C. W. Hughes and S. C. George, *In Vitro* Perfused Human Capillary Networks, *Tissue Eng., Part C*, 2013, **19**, 730–737.
- 11 K.-J. Jang, A. P. Mehr, G. A. Hamilton, L. A. McPartlin, S. Chung, K.-Y. Suh and D. E. Ingber, Human kidney proximal tubule-on-a-chip for drug transport and nephrotoxicity assessment, *Integr. Biol.*, 2013, **5**, 1119–1129.
- 12 R. Baudoin, L. Griscom, M. Monge, C. Legallais and E. Leclerc, Development of a renal microchip for *in vitro* distal tubule models, *Biotechnol. Prog.*, 2007, **23**, 1245–1253.
- 13 K. Jang, K. Sato, K. Igawa, U.-i. Chung and T. Kitamori, Development of an osteoblast-based 3D continuous-perfusion microfluidic system for drug screening, *Anal. Bioanal. Chem.*, 2008, **390**, 825–832.
- 14 B. Altmann, T. Steinberg, S. Giselbrecht, E. Gottwald, P. Tomakidi, M. Bächle-Haas and R.-J. Kohal, Promotion of osteoblast differentiation in 3D biomaterial micro-chip arrays comprising fibronectin-coated poly(methyl methacrylate) polycarbonate, *Biomaterials*, 2011, **32**, 8947–8956.
- 15 M. Skolimowski, M. W. Nielsen, F. Abeille, P. Skafte-Pedersen, D. Sabourin, A. Fercher, D. Papkovsky, S. Molin, R. Taboryski, C. Sternberg, M. Dufva, O. Geschke and J. Emneus, Modular microfluidic system as a model of cystic fibrosis airways, *Biomicrofluidics*, 2012, **6**, 034109.
- 16 D. Huh, B. D. Matthews, A. Mammoto, M. Montoya-Zavala, H. Y. Hsin and D. E. Ingber, Reconstituting Organ-Level Lung Functions on a Chip, *Science*, 2010, **328**, 1662–1668.
- 17 S. Harris and M. Shuler, Growth of endothelial cells on microfabricated silicon nitride membranes for an *in vitro* model of the blood-brain barrier, *Biotechnol. Bioprocess Eng.*, 2003, **8**, 246–251.
- 18 L. M. Griep, F. Wolbers, B. de Wagenaar, P. M. ter Braak, B. B. Weksler, I. A. Romero, P. O. Couraud, I. Vermes, A. D. van der Meer and A. van den Berg, BBB on chip: microfluidic platform to mechanically and biochemically modulate blood-brain barrier function, *Biomed. Microdevices*, 2013, **15**, 145–150.
- 19 L. J. Millet and M. U. Gillette, New perspectives on neuronal development via microfluidic environments, *Trends Neurosci.*, 2012, **35**, 752–761.
- 20 H. J. Kim, D. Huh, G. Hamilton and D. E. Ingber, Human gut-on-a-chip inhabited by microbial flora that experiences intestinal peristalsis-like motions and flow, *Lab Chip*, 2012, **12**, 2165–2174.
- 21 H. J. Kim and D. E. Ingber, Gut-on-a-Chip microenvironment induces human intestinal cells to undergo villus differentiation, *Integr. Biol.*, 2013, **5**, 1130–1140.
- 22 D. Knight, Epithelium-fibroblast interactions in response to airway inflammation, *Immunol. Cell Biol.*, 2001, **79**, 160–164.
- 23 J. Bousquet, P. Chanez, J. Y. Lacoste, G. Barnéon, N. Ghavanian, I. Enander, P. Venge, S. Ahlstedt, J. Simony-Lafontaine, P. Godard and F.-B. Michel, Eosinophilic Inflammation in Asthma, *N. Engl. J. Med.*, 1990, **323**, 1033–1039.

- 24 C. Corrigan, Mechanisms of asthma, *Medicine*, 2008, **36**, 177–180.
- 25 J. W. Wilson and T. L. Bamford, Assessing the Evidence for Remodelling of the Airway in Asthma, *Pulm. Pharmacol. Ther.*, 2001, **14**, 229–247.
- 26 A. A. Humbles, C. M. Lloyd, S. J. McMillan, D. S. Friend, G. Xanthou, E. E. McKenna, S. Ghiran, N. P. Gerard, C. Yu, S. H. Orkin and C. Gerard, A Critical Role for Eosinophils in Allergic Airways Remodeling, *Science*, 2004, **305**, 1776–1779.
- 27 G. J. Gleich, Mechanisms of eosinophil-associated inflammation, *J. Allergy Clin. Immunol.*, 2000, **105**, 651–663.
- 28 J. M. Hohlfeld, A. Schmiedl, V. J. Erpenbeck, P. Venge and N. Krug, Eosinophil cationic protein alters pulmonary surfactant structure and function in asthma, *J. Allergy Clin. Immunol.*, 2004, **113**, 496–502.
- 29 C. E. Brightling, A. J. Ammit, D. Kaur, J. L. Black, A. J. Wardlaw, J. M. Hughes and P. Bradding, The CXCL10/CXCR3 Axis Mediates Human Lung Mast Cell Migration to Asthmatic Airway Smooth Muscle, *Am. J. Respir. Crit. Care Med.*, 2005, **171**, 1103–1108.
- 30 R. Saunders, S. Siddiqui, D. Kaur, C. Doe, A. Sutcliffe, F. Hollins, P. Bradding, A. Wardlaw and C. E. Brightling, Fibrocyte localization to the airway smooth muscle is a feature of asthma, *J. Allergy Clin. Immunol.*, 2009, **123**, 376–384.
- 31 C. H. Wang, C. D. Huang, H. C. Lin, K. Y. Lee, S. M. Lin, C. Y. Liu, K. H. Huang, Y. S. Ko, K. F. Chung and H. P. Kuo, Increased circulating fibrocytes in asthma with chronic airflow obstruction, *Am. J. Respir. Crit. Care Med.*, 2008, **178**, 583–591.
- 32 K. Nihlberg, K. Larsen, A. Hultgardh-Nilsson, A. Malmstrom, L. Bjermer and G. Westergren-Thorsson, Tissue fibrocytes in patients with mild asthma: a possible link to thickness of reticular basement membrane?, *Respir. Res.*, 2006, **7**, 50.
- 33 R. A. Reilkoff, R. Bucala and E. L. Herzog, Fibrocytes: emerging effector cells in chronic inflammation, *Nat. Rev. Immunol.*, 2011, **11**, 427–435.
- 34 R. J. Phillips, M. D. Burdick, K. Hong, M. A. Lutz, L. A. Murray, Y. Y. Xue, J. A. Belperio, M. P. Keane and R. M. Strieter, Circulating fibrocytes traffic to the lungs in response to CXCL12 and mediate fibrosis, *J. Clin. Invest.*, 2004, **114**, 438–446.
- 35 R. M. Strieter, B. N. Gomperts and M. P. Keane, The role of CXC chemokines in pulmonary fibrosis, *J. Clin. Invest.*, 2007, **117**, 549–556.
- 36 K. C. Chang, C. W. Lo, T. C. Fan, M. D. Chang, C. W. Shu, C. H. Chang, C. T. Chung, S. L. Fang, C. C. Chao, J. J. Tsai and Y. K. Lai, TNF-alpha mediates eosinophil cationic protein-induced apoptosis in BEAS-2B cells, *BMC Cell Biol.*, 2010, **11**, 6.
- 37 C. Palmqvist, A. J. Wardlaw and P. Bradding, Chemokines and their receptors as potential targets for the treatment of asthma, *Br. J. Pharmacol.*, 2007, **151**, 725–736.